Local Substructures of Water Studied by Transient Hole-Burning Spectroscopy in the Infrared: Dynamics and Temperature Dependence

R. Laenen,* C. Rauscher, and A. Laubereau

Physik-Department E11, Technische Universität München, D-85748 Garching, Germany

Received: January 6, 1998; In Final Form: April 7, 1998

The spectral substructure of the OH-stretching band of the isotopic mixture HDO in D_2O is demonstrated in the temperature range of 273−343 K, using two-color IR spectroscopy with tuneable subpicosecond and picosecond pulses. We derive from time-resolved spectra three major components peaked at approximately 3330 cm^{-1} (I), 3400 cm^{-1} (II), and 3450−3500 cm^{-1} (III). In contrast to I and II, species III displays a distinct temperature dependence of position and bandwidth. The latter varies in the range 90−140 cm^{-1}, representing inhomogeneous broadening above 290 K, as indicated by novel hole-burning observations with a hole width of 45 cm^{-1} and a lifetime of the holes of ≈1 ps. The species I−III are also characterized by different values of the reorientational time constant in the range of 3−15 ps, depending on temperature, and are attributed to different preferred local environments in the hydrogen-bonded network. Component I observed with decreasing amplitude up to 343 K is close to a frequency characteristic for the ice structure I_h and provides evidence for approximately tetrahedral local geometries in liquid water. From the measured cross-relaxation among the spectral species, a structural relaxation time of 1.5−0.8 ps is deduced in the range 273−343 K. The populational lifetime of the first excited state of the OH-stretching vibration of component II is measured to be 1.0 ± 0.2 ps at room temperature.

1. Introduction

Water as the most important liquid exhibits special properties owing to its ability to form a hydrogen-bonded network with striking consequences for the biosphere, e.g., the anomalous melting and boiling points of this liquid. For a detailed understanding, numerous experimental and theoretical investigations were conducted on water.[1] The structure and the structural dynamics were examined by neutron,[2] Rayleigh,[3] and X-ray[4] scattering, while the reorientation of water molecules was studied by NMR[5] and dielectric relaxation[6] measurements. Very recently the fast intermolecular motion has been elucidated by measurements on the sub-100-fs time scale using the Raman-induced Kerr effect.[7] Existing spectroscopic methods alternatively offer large spatial or temporal resolution, while both features are required to investigate the dynamics of local structures. As a result the available information on the dynamics of water refer a structural average and vice versa, and the complexity of the hydrogen-bonded liquid may not be fully known yet.

A possibility to recognize different water structures with the necessary time resolution is offered by the OH-stretching vibration that may serve as a local probe for hydrogen bonding.[8] The OH mode exhibits a red-shift and noteable broadening with increasing strength of the hydrogen bond accompanied also by an increasing absorption cross section. Such features are utilized by infrared[9,10] and Raman[11] spectroscopic investigations in order to identify different structural components applying also temperature or pressure changes. To obtain information on molecular dynamics, time-resolved anti-Stokes Raman[12,13] or infrared techniques[14] were demonstrated to be powerful tools. Improved versions of the pump−probe-spectroscopy with two independently tunable IR pulses[15,16] and with polarization resolution[17,18] provide detailed spectroscopic insight. In fact, transient spectroscopy on the isotopic mixture HDO in D_2O delivered evidence for three distinct spectral components in the range 3340−3520 cm^{-1} at room temperature.[19] Owing to the limited time resolution of 11-ps pulses, the dynamics of the various components could not be measured. In the present investigation with shorter and almost bandwidth-limited infrared pulses, we are able to substantiate the earlier findings and obtain novel information on the cross-relaxation among the different structural components in the temperature range 273 K (undercooled liquid) to 343 K. We also observe for the first time spectral holes that occur in the OH-stretching band of HDO. The results are supported by different values for the reorientation times of the three major components. Very recently evidence for the existence of two structural components of water was reported[20] from measurements of reorientational time constants. The physical picture derived from our data is different and more detailed.

2. Experimental Section

Our experimental system was discussed in detail elsewhere[21] and is only briefly described here. We start with a pulsed, Kerr-lens modelocked Nd:YLF laser for the synchronous pumping of two optical parametric oscillators in parallel. Single-pulse selection, frequency down-conversion, and amplification of the OPO outputs are carried out in subsequent optical parametric amplifier stages. In this way, independently tunable excitation and probing pulses of ≥450 fs duration and spectral width ≤35 cm^{-1} are generated in the range 1600−3700 cm^{-1}.[22] For the major part of the investigations, longer pulses were used with pulse durations of 2 and 1 ps for pump and probe, respectively. The latter pulses are also close to the Fourier transform limitation as indicated, e.g., by spectral widths of 8 cm^{-1} for the 2-ps excitation pulses and accomplish superior spectral resolution.

10.1021/jp980667w CCC: $15.00
Published on Web 10/27/1998

The data discussed in the following refer to the longer pulse durations if use of the subpicosecond pulses is not explicitly stated.

Two-color pump−probe absorption spectroscopy is carried out with moderate pump energies of several microjoules and a frequency setting within the full width of the OH band, producing small depletions of the vibrational ground state of a few percent only. Probing energies are reduced to a few nanojoules, 3 orders of magnitude below the excitation values. The energy transmission $T(\nu)$ of the probing pulse through the excited sample is measured for parallel (||) and perpendicular (⊥) polarization with respect to the linearly polarized pump and compared with the sample transmission $T_0(\nu)$ for the blocked excitation beam. The resulting relative transmission changes $\ln(T/T_0)_{||,\perp}$ for variable probe frequency ν and probe delay time t_D are used in the following as the relevant signal quantities, from which an isotropic signal amplitude, $\ln(T/T_0)_{is} = (\ln(T/T_0)_{||} + 2\ln(T/T_0)_{\perp})/3$, an anisotropic signal $\ln(T/T_0)_{anis} = \ln(T/T_0)_{||} - \ln(T/T_0)_{\perp}$, and the induced dichroism $\ln(T/T_0)_{anis}/3\ln(T/T_0)_{is}$ can be deduced.[17] The isotropic signal delivers information on the molecular number densities and population dynamics, while the temporal evolution of the induced dichroism is governed by the time constant τ_{or} (second-order reorientational correlation time, $l = 2$), only if population redistribution does not contribute to the loss of induced anisotropy. The zero setting of the delay time scale (maximum overlap between pump and probing pulses) is determined by a two-photon absorption technique in independent measurements with an accuracy of better than ±0.2 ps.[23]

The sample solutions are prepared from commercially available deuterated water (99.9%) and tridistilled water without further purification. An HDO concentration of 0.8 M is chosen for a sample thickness of 100 μm corresponding to a minimum sample transmission of 0.12 at 3400 cm^{-1} (T = 298 K). The measurements are performed in the temperature range 273−343 K (±0.5 K).

3. Experimental Results

Conventional IR absorption data are taken with a a commercial Fourier transform spectrometer and are corrected for the absorption of the solvent D_2O so that essentially the HDO contribution is retained. An example for 298 K is shown in Figure 1b (solid line, right-hand ordinate scale). A broad, structureless absorption occurs around 3400 cm^{-1}, accompanied by additional features in the red wing of the band.

Transient spectra for excitation in the red edge of the OH band are presented in Figure 1 for zero delay time and three different temperatures. The isotropic signal component is plotted representing population changes. For the undercooled liquid and a pump frequency of 3330 cm^{-1} (Figure 1a, 273 K) the transient bleaching is governed by a component I (dash−dotted curve) close to ν_{Pu} and another contribution II at 3400 cm^{-1} (dashed line). Two further weak components may be recognized at this delay time in the wings at 3260 cm^{-1} (dash−dot−dotted, I′) and around 3500 cm^{-1} (component III, long-dashed). The induced absorption peaked at 2920 and 3160 cm^{-1} will be discussed below. When the temperature is adjusted to room temperature (Figure 1b), the bleaching feature is considerably different; our analysis suggests that the components I−III now exhibit similar amplitudes with a small shift of III to 3450 cm^{-1}, and an additional narrow band at the excitation frequency (dotted line) referred to as a spectral hole. The induced absorption in the red part below 3300 cm^{-1} is almost unchanged. Further increase of the temperature to 343 K and adjusting ν_{Pu} = 3380 cm^{-1} yields the spectrum depicted in Figure 1c. Again a transient spectral hole (dotted) can be deduced from the data while component III (long-dashed) clearly dominates the bleaching. Contribution I (dash−dotted), on the other hand, is insignificant. The induced absorption below 3300 cm^{-1} is once more broad and featureless.

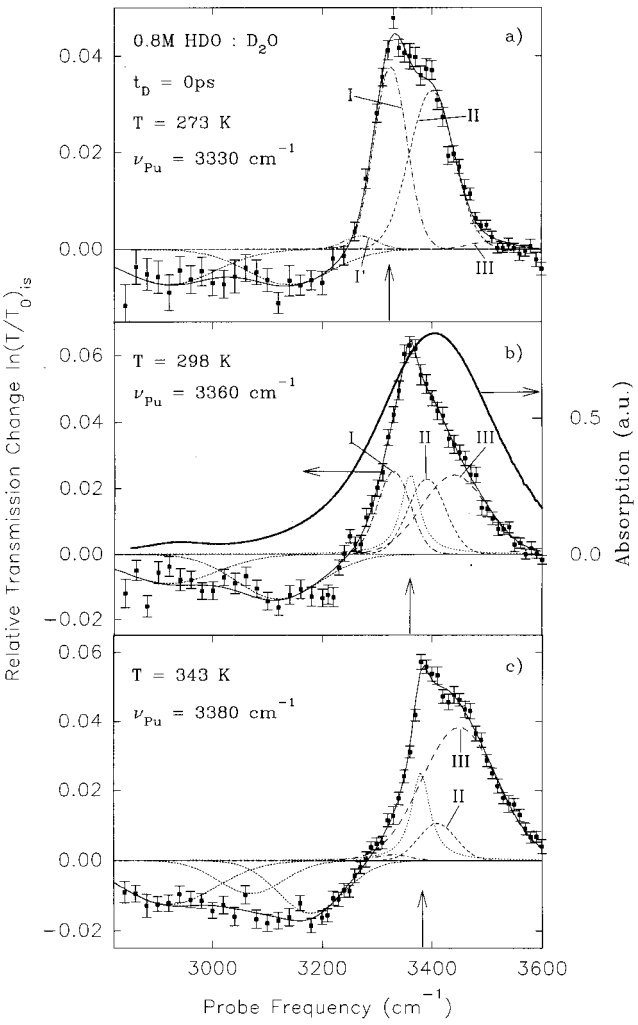

Figure 1. Transient spectra (isotropic signal) for t_D = 0 ps and excitation in the red wing of the OH band at three temperature values: 273 K (a), 298 K (b), and 343 K (c). The thick solid line in (b) denotes the measured conventional absorption band of HDO (right-hand ordinate scale); experimental points; the calculated thin lines indicate the analysis of the transient band shapes (thin full line) in terms of the major spectral components I−III (dash−dotted, broken, long-dashed) with Gaussian shape and a Lorentzian spectral hole contribution (dotted); the pump frequencies are indicated in the figure by vertical arrows.

Spectra for excitation around the peak position of the OH band are depicted in Figure 2 at t_D = 0 and three temperature values. At T = 273 K (Figure 2a), the isotropic signal amplitude is mainly governed by component II (dashed curve) while I and III give only minor contributions to the wings of the bleaching and a spectral hole is not observed. The induced absorption around 3160 cm^{-1} shows up again as a broad structure. When changing to room temperature (Figure 2b), the spectrum looks different and a spectral hole (dotted) can be inferred from the data in addition to the components I−III. Further increase of the temperature to 343 K leads to the band shape depicted in Figure 2c. The main contribution to the bleaching is assigned to component III (long-dashed) and a spectral hole (dotted), while the other species display smaller amplitudes.

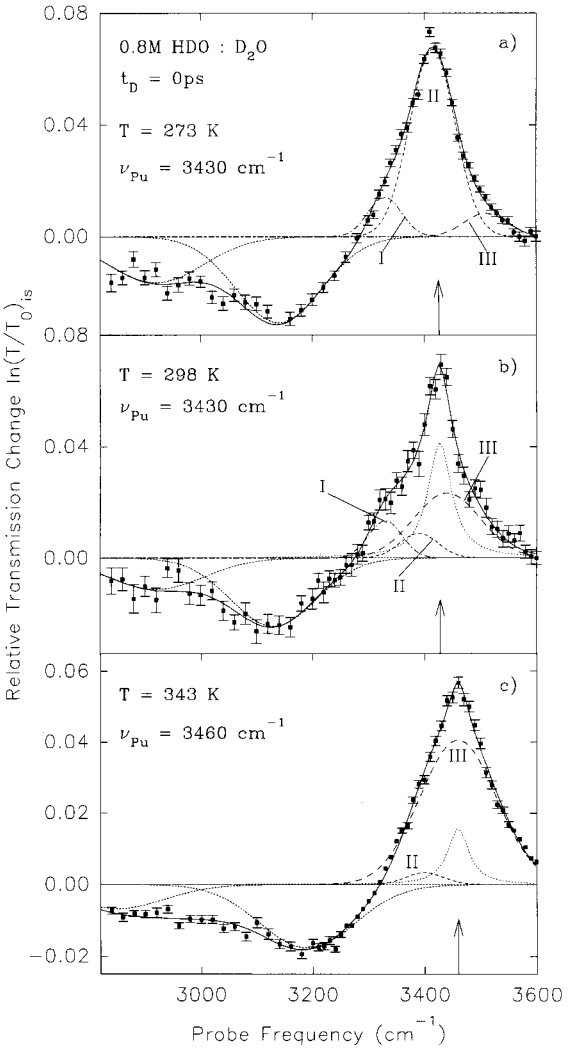

Figure 2. Same as Figure 1 for excitation in the center of the OH band; the temperature values and pump frequencies are indicated in the figure.

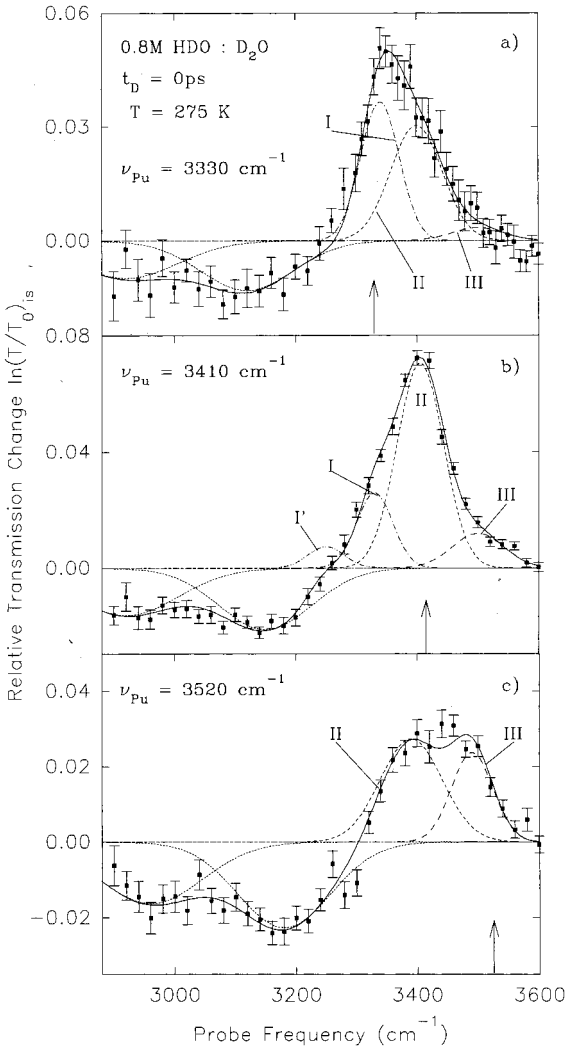

Figure 3. Same as Figure 1, but for constant temperature $T = 275$ K and three different frequency positions of the excitation pulse (note vertical arrows): 3330 cm^{-1} (a), 3410 cm^{-1} (b), and 3520 cm^{-1} (c). Note different ordinate scales.

The dependence on excitation frequency is illustrated by the data of Figure 3 taken at 275 K and zero delay time. With the pump pulse tuned resonantly to the position of component I (Figure 3a), the latter (dash−dotted) dominates the bleaching, but with a large amplitude also of II and neglible contribution of III. Alternatively exciting at the position of II (Figure 3 b) accomplishes a large bleaching amplitude of II and smaller contributions of I and III, while the bleaching peak and the induced absorption below 3250 cm^{-1} gain somewhat in amplitude (note different ordinate scales). Tuning the excitation to the blue wing of the OH absorption (Figure 3c), we find large amplitudes of species II and III while the contribution of I is negligible. We notice that a spectral hole contribution is not found in Figure 3 for 275 K.

An example for the time evolution of the spectra is presented in Figure 4, which refers to pumping at 3520 cm^{-1} in the blue wing of the OH band, and three values of probe delay at 275 K are given. The bleaching feature is decomposed again into the dominant contributions of components II and III (dashed and long-dashed curves, respectively), the amplitudes depending on time. At −1 ps the preferentially pumped species III is seen to be dominant (Figure 4 a), while spectral relaxation obviously transfers population to component II that prevails at $t_D = 1$ ps (Figure 4c). The induced absorption around 3180 cm^{-1}, on the other hand, representing excited-state population, decays simultaneously (Figure 4b,c).

Some data on the temporal evolution of the signal amplitudes at fixed probing frequencies are shown in Figure 5. The liquid at room temperature (298 K) is investigated with preferential excitation of component II at $\nu_{Pu} = 3410$ cm^{-1} in the center of the OH absorption, using pump and probing pulses of 450 fs. Adjusting the probing at the same frequency, $\nu = \nu_{Pu}$ (Figure 5 a), we observe first an increase of the isotropic sample transmission within experimental time resolution, followed by a rapid decay. The asymmetry of the signal curve clearly shows the finite response of the sample molecules representing population dynamics. From the later part of the signal decay ($t_D > 1$ ps), a time constant of 1.2 ± 0.2 ps is obtained (see below). The signal amplitude does not completely recover to the initial value indicating a new thermal equilibrium. The corresponding induced dichroism is depicted in Figure 5b. The signal decay starts at negative delay times from a level close to the theoretical maximum of 0.4 and indicates a rather slow reorientational motion with $\tau_{or}(II) = 10 \pm 3$ ps at 298 K. When the induced absorption at 3150 cm^{-1} (Figure 5c) is probed, a fast decrease of the signal is noticed, which is followed by a

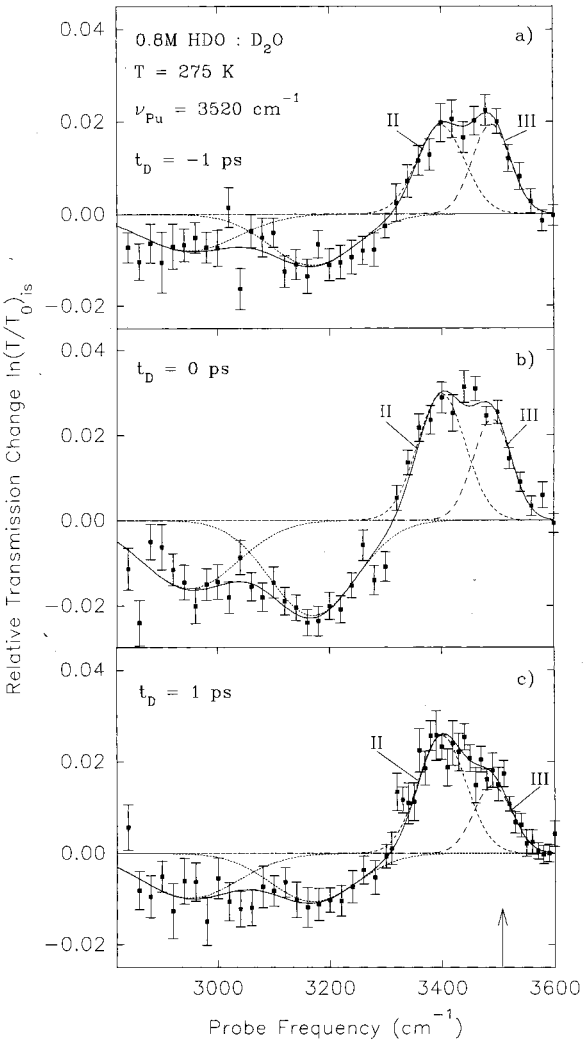

Figure 4. Same as Figure 1, but for constant temperature $T = 275$ K, constant excitation frequency of 3520 cm^{-1} (vertical arrow) and three temporal positions of the probing pulse: $t_D = -1$ ps (a), $t_D = 0$ (b), and $t_D = 1$ ps (c).

relaxation to the initial amplitude; from the later part of the decay curve (>1 ps) a time constant of $T_1 = 1.0 \pm 0.2$ ps is deduced.

4. Data Analysis

The transient spectra can be described by computed data assuming Gaussian shapes for the various spectral components while the spectral hole is assumed to be Lorentzian. The solid lines in Figures 1−4 are the results of a fitting procedure using the Levenberg−Marquardt algorithm.[24] Three major spectral species are deduced self-consistently from a fitting procedure for the manifold of isotropic and anisotropic transient spectra taken at various delay times and excitation frequencies within the full width of the OH band of HDO at a certain temperature value. A minor contribution denoted with I′ at 3260 cm^{-1} has in addition to be included at lower temperatures. Only the amplitudes of the components are allowed to change with delay time and excitation frequency. As a fourth major contribution, the spectral hole positioned at the pump frequency is included for temperatures above 290 K and in the frequency band of species III, since a hole was not observed at lower temperatures.

The results of five sets of measurements in the range 273−343 K are presented in Figure 6. The peak positions and the spectral widths (fwhm) of the spectral species I−III are plotted

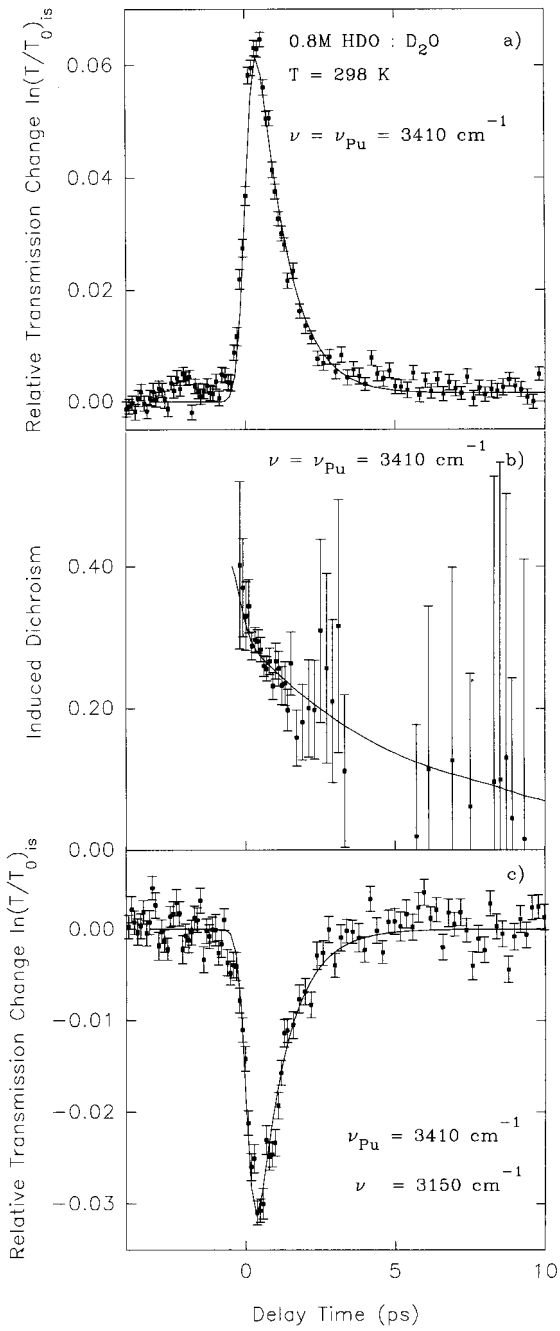

Figure 5. Signal transients at fixed probing frequencies and excitation at 3410 cm^{-1}, measured with pulses of 450 fs at $T = 298$ K: (a) isotropic signal versus delay time for $\nu = \nu_{Pu} = 3410$ cm^{-1}; (b) induced dichroism for $\nu = \nu_{Pu} = 3410$ cm^{-1}; (c) isotropic signal at 3150 cm^{-1}; experimental points, calculated curves; a lifetime of the OH-stretching vibration of $T_1 = 1.0 \pm 0.2$ ps and a reorientation time of $\tau_{or} = 10 \pm 3$ ps are determined, considering in the model calculations also for spectral relaxation; see text.

in parts a and b of Figure 6, respectively. While components I and II with the strongest red-shift (of the OH mode in comparison to the monomeric HDO) exhibit almost no temperature dependence, we find for species III a decrease from 3510 cm^{-1} at 273 K to 3450 cm^{-1} for temperatures above 290 K. A similiar behavior is found for the spectral widths; that of I appears temperature independent with a value of 70 ± 5 cm^{-1}, II exhibits a slight narrowing from 95 ± 5 cm^{-1} to 80 ± 5 cm^{-1}, and component III with the smallest red-shift and consequently weakest H-bonds displays significant broadening from 90 ± 5 cm^{-1} at 273 K to 140 ± 7 cm^{-1} above 290 K.

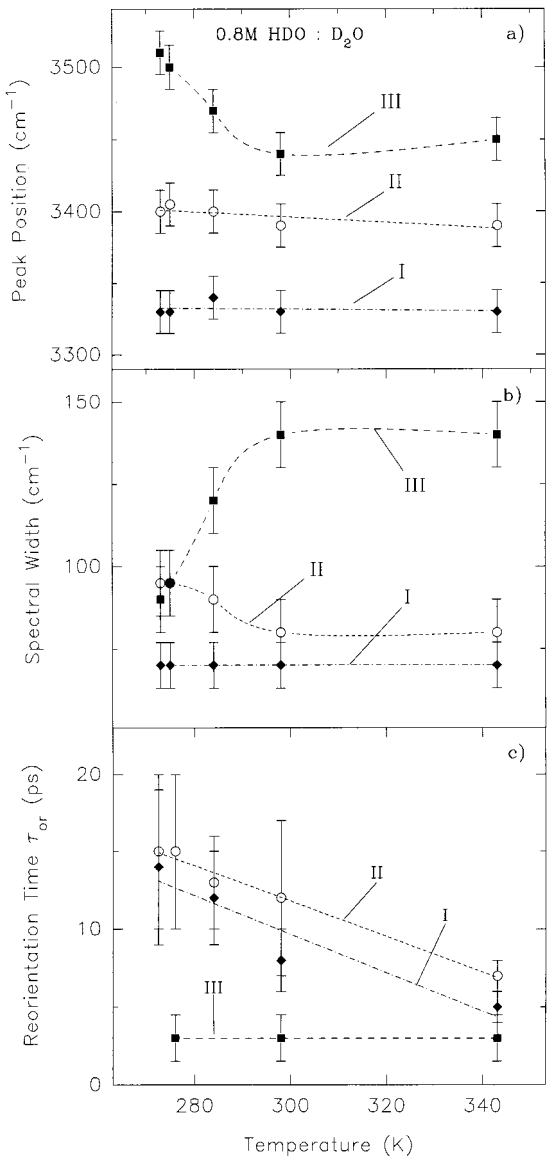

Figure 6. Results of the decomposition of the measured transient spectra: the peak positions (a), spectral widths (fwhm) (b), and reorientation times (c) of three prominent spectral components I−III, attributed to different local structures of water, as a function of temperature; experimental points; the lines are drawn as a guide for the eye.

The increased bandwidth is consistent with the occurrence of spectral holes in contribution III at higher temperatures, suggesting inhomogeneous broadening of the latter. The different character of the spectral species is supported by results on the reorientation time of the OH group of HDO depicted in Figure 6c. The time constants of I and II shorten from approximately 15 ps at 273 K to 5 and 7 ps, respectively, at 343 K, while species III exhibits fast reorientation with $\tau_{or} = 3 \pm 1.5$ ps, approximately independent of temperature.[25]

The time-dependent measurements are simulated by a rate equation model that is based on a simplified four-level system and takes into account the two orthogonal polarizations of the probing process with respect to the excitation.[26] The finite lifetime of the induced transition dipole moments is neglected (dephasing time $T_2 \ll 1$ ps). The four-level scheme considers the vibrational ground state of the OH-stretching mode (0), first excited level $v = 1$ (1) of the respective spectral component(s) directly pumped by the excitation pulse, and population redistribution to an intermediate state (2) representing the other

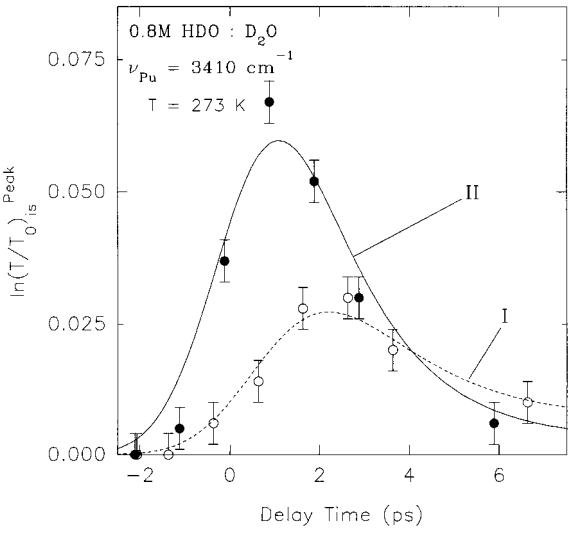

Figure 7. Spectral relaxation within the OH-stretching band of HDO in D_2O at 273 K; the peak amplitudes (isotropic signal) of species I (filled circles, solid line) and II (hollow circles, dashed curve) are plotted versus probe delay, as derived from the decomposition of the measured transient spectra with excitation at 3410 cm^{-1}; experimental points, calculated lines.

spectral components involved in the dynamics and grouped together in only one level. Population decay out of levels 1 and 2 finally leads to a thermally modified, long-lived ground state 3. Vibrational relaxation results in a small temperature and pressure increase of the excited sample on the picosecond time scale with a corresponding red-shift and broadening of the OH band. This heating of the excited sample is dissipated later on in much longer times compared to our observation interval. The redistribution time τ_s from level 1 to 2 is consistently attributed to spectral relaxation of the primarily excited molecules selected in their specific environment by the frequency position of the pump pulse. The reverse process $2 \rightarrow 1$ is included considering detailed balance, the relative statistical weights of the two levels treated as a fitting parameters. More specificly, the spectral redistribution process is interpreted as structural relaxation of the fluctuating H-bonding environments. A contribution of intermolecular vibrational energy transfer to the redistribution process appears to be negligible because of the dilution of HDO in the solvent D_2O and the large frequency mismatch between OH- and OD-stretching modes. The populations of levels 1 and 2 are assumed to decay with time constants τ_{13} and τ_{23}, respectively. The simplification $\tau_{13} \simeq \tau_{23} = T_1$ is introduced in general in the data analysis. The last time constant represents an average population lifetime of the OH-stretching mode of HDO.

T_1 is determined from the relaxation of the excited-state population (see Figure 5c) to be 1.0 ± 0.2 ps for preferential excitation at 3410 cm^{-1} of species II and taking into account the spectral redistribution process. The ground-state recovery derived from our time-dependent data proceeds with the same T_1 values (cf. Figure 5a,b) indicating that further intermediate states (between 2 and 3) need not be considered in the population relaxation.

Some data for the spectral reshaping described by the redistribution time τ_s are presented in Figure 7 for excitation at 3410 cm^{-1} and 273 K. The relative amplitudes (peak value of isotropic signal) of species I and II as obtained from the spectral decomposition of the transient spectra are plotted versus delay time. It is interesting to see that the resonantly pumped species II (filled circles, solid line) rises rapidly, close to experimental

time resolution, and decays via time constants τ_s and $\tau_{13} \simeq T_1$, the latter being known from the data of Figure 5c. Component I (hollow circles, dashed curve), on the other hand, is pumped by the excitation pulse only to a small extent and grows notably delayed because of the spectral redistribution process. Comparison with the rate equation model (calculated lines in the figure) yields the value $\tau_s = 1.5 \pm 0.5$ ps, which is interpreted as the structural relaxation time of water at 273 K. Somewhat shorter numbers of $\tau_s = 1.0 \pm 0.4$ ps and 0.8 ± 0.4 ps are deduced at 298 and 343 K, respectively (data not shown). The data for species III suffer from a small amplitude level and the limited measuring accuracy and are not shown in Figure 7.

The lifetime of the transient holes is determined to be $\tau_h = 1 \pm 0.5$ ps in the temperature range 298−343 K, quite similar to the structural relaxation time. In fact, the hole lifetime (originating from the observation of spectral relaxation) may be again assigned to structural relaxation. Molecules of species III may experience a variation of their surroundings changing the H-bonding with a corresponding shift of the OH frequency decreasing the hole amplitude. Furthermore we believe to see in the transient spectra of Figure 3 ($T = 275$ K) almost no rearrangement between species I and III (Figure 3a,c), although excitation of component II results in equal bleaching amplitudes for I and III (Figure 3b). This selectivity in interaction disappears for temperatures ≥284 K and could be explained by the increasing flexibility of the water network with rising temperature.

5. Discussion of the Spectral Components

Three major spectral components I−III are derived from the transient spectra and assigned to distinct structural environments determining the frequency position of the OH vibration in semiquantitative agreement with earlier findings.[19] The spectral observations are consistent with MD computations that predicted three classes of sites in the water network.[27] Species I is located at a frequency close to the OH frequency of HDO for the ice structure I_h involving at least four strong H-bonds and possibly small bond angles, as suggested by a comparison of the peak position with data of conventional infrared[28] and Raman spectroscopy[29] and in accordance with the slow orientational motion (see Figure 6c). Evidence for an approximately tetrahedral local geometry in liquid water in the measuring range 273−343 K is obtained in accordance with MD simulations.[30] Partial formation of H bridges will lead to a higher OH frequency (structure II), a component that has been also reported earlier from Raman investigations.[29] The spectral component III obviously corresponds to an even weaker H-bonding situation and is tentatively assigned to molecules with bifurcated H-bonds as concluded previously from the Raman spectrum of HDO, where a spectral feature at ≃3435 cm^{-1} was found at room temperature[31] and attributed to bifurcated H-bonds.[32,33] It should be noted that a possible substructure of species III with overlapping components and different temperature dependencies cannot be excluded from the present data. Components close to the frequency positions of the species II and III determined here can be also estimated from results for the OD band of HDO.[34] Our data on three major species I, II, and III do not exclude the existence of further (weaker) components. It is recalled that in principle all of the 12 possible bonding configurations of HDO[35] may contribute to the overall OH band with respective Raman and/or IR activity.

The decrease of sample transmission around 3160 cm^{-1} after excitation within the OH band is attributed to excited-state absorption (ESA) of probing transitions $v = 1 \rightarrow v = 2$. The peak position of the approximately 180 cm^{-1} wide ESA band varies between 3120 and 3200 cm^{-1}, depending on excitation frequency and temperature. The average value of the anharmonic shift of the OH-stretching vibration is estimated to be 240 ± 20 cm^{-1}. The number is consistent with the earlier result of 270 ± 20 cm^{-1} of ref 19 and in satisfactory accordance with results for other hydrogen-bonded systems, e.g., 210 cm^{-1} for a dimer in a polymer matrix[17] and 230 cm^{-1} for ethanol oligomers in liquid solution.[37] The anharmonic shifts seem to vary with the strength of the H-bonding.

A further component shows up in induced absorption at 2940 ± 20 cm^{-1} (see Figures 3, 4) that is tentatively assigned to an overtone of the bending mode of HDO. A corresponding feature is found in the conventional IR spectrum at 2960 cm^{-1} (compare Figure 1b). The induced absorption presents evidence that an excited level of the bending vibration is populated by energy transfer from the stretching mode. The relaxation channel was previously suggested for water vapor.[38] The induced absorption at 2940 cm^{-1} displays a pronounced isotropic character in contrast to the anisotropic excited-state absorption around 3160 cm^{-1}. This notion supports the conclusion that the signal around 2940 cm^{-1} involves a secondary process with loss of orientational information, e.g., energy transfer.

Our results on the spectral substructure of the OH absorption are consistent with the band shape in the conventional IR spectrum of HDO. For a quantitative description of the latter, an additional weaker component at 3270 cm^{-1} is required below 300 K that shows up also in the transient spectrum in the same temperature range, denoted with I′. This component is located at a frequency determined for a special ice conformation from Raman spectroscopic investigations.[29] A further contribution to the overall OH absorption band of HDO is noticed at 3260 cm^{-1}; it is believed that the latter do not represent OH-stretching transitions and were recently assigned to an overtone of the OH-bending mode and a combination band, respectively.[19] Increase of temperature reduces significantly the contribution of components I and II, while species III dominates the conventional absorption band above 290 K.

6. Discussion of the OH Lifetime and Structural Relaxation

It is interesting to compare our value of 1.0 ps for the population lifetime in the center of the OH band of HDO with other data. From saturation studies with 110-ps laser pulses, the lifetime of the OH mode was stated to be in the range 0.3−0.6 ps.[39] The numbers refer to a simple two-level model used in the data analysis and represent an effective time constant including spectral relaxation and ground-state recovery. A quantitative comparison is not possible because of the distinct heating of the molecular environment expected for a 110-ps pulse. Very recently Woutersen et al.[20] reported a vibrational lifetime of ≈0.7 ps derived from one-color IR measurements with 250-fs pulses at room temperature. Since spectral relaxation was not discussed by these authors, the time constant may be interpreted as an effective population lifetime with a contribution of the spectral redistribution process included in the reported value. The T_1 of the OH-stretching mode of H-bonded water molecules may be also compared to the population lifetime of the same vibration of ethanol oligomers in solution of CCl_4. For this system a value of 1.7 ± 0.3 ps was found at room temperature[37] while ethanol monomers[40] exhibit a considerably larger time constant of 8 ± 1 ps. Obviously in this system hydrogen bonding notably reduces the lifetime of the OH vibration, as is also suggested for HDO by a comparison with results for H_2O monomers.[41]

Our data on the reorientation time (Figure 6c) are at variance with the results of Woutersen et al.[20] for HDO at room temperature. These authors report a different behavior of the reorientational motion measured at three spectral positions within the OH band in a one-color experiment with pulses of 250 fs and spectral width of 70−100 cm^{-1}. At 3320 cm^{-1} a singly exponential decay of the induced dichroism with a time constant of 13 ps was measured, whereas at 3400 and 3500 cm^{-1} biexponential relaxation with time constants of 0.7 and 13 ps was reported (experimental accuracy not stated). The authors concluded that with respect to the orientational dynamics two distinct species of liquid water molecules exist. Our data of Figure 6c indicate that three single reorientational time constants can be unambiquously assigned to three dominant species I−III with values of 3 ± 1.5 ps, 8 ± 2 ps, and 12 ± 5 ps, respectively, at 298 K. The data of Figure 5b measured with pulses of 460 fs readily show that a fast signal contribution cannot be overlooked in the measurement, since the signal amplitudes start at the maximum theoretical value of 0.4. The different findings of ref 20 may be related to the larger bandwidth of the pulses used there so that a superposition of spectral species is observed. Our data allow the conclusion that the reorientational motion is slowed with increasing strength of the hydrogen bonding, i.e., red-shift of the spectral species. Component III with smallest red-shift reorients most rapidly with ≈3 ps in accordance with the reorientation time of water monomers in various inert solvents of approximately 2 ps.[41]

Our findings for τ_s and τ_h may be compared with results of computer simulations for water. Values between 1 and 2 ps are stated for the average lifetime of a hydrogen bond by different authors[42−44] in satisfactory agreement with our experimental values. It is also interesting to compare with the frequency shift correlation function of the vibrational modes of water obtained from MD computations.[45] Recently a slower component of this function with an exponential time constant of 0.8 ps was predicted for HDO in D_2O at 300 K and a density of 1.1 g/cm^3 (pressure of ≈2 kbar). The existence of the slow component is a necessary prerequisite for the observation of spectral holes and the spectral relaxation time τ_s reported here.

The faster component of the frequency shift correlation function with $\tau_c = 50$ fs[45] represents rapid fluctuations that determine the spectral bandwidths of the spectral species and of the spectral holes. The value of τ_c suggests quasi-homogeneous broadening, $\tau_c\Gamma_i < 0.5$, of species I, II and the spectral holes of III, introducing here the respective halfwidths Γ_i (hwhm). In fact, no evidence for hole burning was found for species I and II in our measurements. The measured full width of 45 ± 5 cm^{-1} (fwhm) of the spectral holes within species III above 290 K can be compared with transient hole-burning data for associated ethanol[37] and for hydrogen-bonded OH groups in a polymer matrix ("dimers").[46] In the first case of a liquid solution studied with ≈1-ps pulses a similiar hole width is deduced from the transient spectra while for the dimers in the solid matrix investigated with ≈10-ps pulses the value is larger by a factor of approximately 2 at room temperature, decreasing strongly for lower temperatures. The differences are not fully understood at the present time and necessitate further investigation.

7. Conclusions

We have observed for the first time transient spectral holes in the OH band of HDO in the temperature range from 298 to 343 K with a lifetime of approximately 1 ps. Spectral relaxation assigned to structural dynamics proceeds with a time constant of ≈1.5−0.8 ps, depending on temperature. Three major spectral components are derived from the time-resolved spectra: a species I that is located at 3330 cm^{-1}, close to the absorption of ice I_h, providing evidence for an approximately tetrahedral local geometry in liquid water, a component II with moderately strong H-bonding at 3400 cm^{-1}, and a weakly bonded structure III peaked between 3450 and 3500 cm^{-1}. Species III is possibly related to bifurcated hydrogen bonds and exhibits temperature-dependent broadening up to 140 cm^{-1} while the width of the spectral holes observed within this component is measured to be 45 cm^{-1}. The different character of the three major species is supported by different values of the reorientation time of the OH axis of HDO in the respective environments. The population lifetime of the OH mode of species II is determined to be 1.0 ± 0.2 ps at room temperature.

The authors acknowledge experimental assistance of K. Simeonidis in part of the investigations, and R.L. thanks the Deutsche Forschungsgemeinschaft (DFG) for financial support.

References and Notes

(1) Franks, F. *Water, A Comprehensive Treatise*; Plenum Press: New York, 1972.
(2) Teixeira, J.; Bellissent-Funel, M.-C.; Chen, S. H. *J. Phys.: Condens. Matter* **1990**, *2*, SA105.
(3) Conde, O.; Teixeira, *J. Mol. Phys.* **1984**, *53*, 951.
(4) A. H. Narten and H. A. Levy in ref 1Radnai, T.; Ohtaki, H. *Mol. Phys.* **1996**, *87*, 103.
(5) Meiboom, S. *J. Chem. Phys.* **1961**, *34*, 375.
(6) Barthel, J.; Bachhuber, K.; Buchner, R.; Hetzenauer, H. *Chem. Phys. Lett.* **1990**, *165*, 369.
(7) Foggi, P.; Bellini, M.; Kien, D. P.; Vercuque, I.; Righini, R. *J. Phys. Chem.* **1997**, *A101*, 7029.
(8) Schuster, P.; Zundel, G.; Sandorfy, C. *The Hydrogen Bond*; North-Holland: Amsterdam, 1976; Vols. I−III.
(9) van Thiel, M.; Becker, E. D.; Pimentel, G. C. *J. Chem. Phys.* **1957**, *27*, 486.
(10) Marechal, Y. *J. Chem. Phys.* **1991**, *95*, 5565.
(11) Walrafen, G. E. *J. Chem. Phys.* **1964**, *40*, 3249. Walrafen, G. E. *J. Chem. Phys.* **1967**, *47*, 114. Walrafen, G. E. *J. Phys. Chem.* **1990**, *94*, 2237.
(12) Laubereau, A.; von der Linde, D.; Kaiser, W. *Phys. Rev. Lett.* **1972**, *28*, 1162.
(13) Hofmann, M.; Graener, H. *Chem. Phys.* **1996**, *206*, 129.
(14) Spanner, K.; Laubereau, A.; Kaiser, W. *Chem. Phys. Lett.* **1976**, *44*, 88. Heilweil, E. J.; Casassa, M. P.; Cavangh, R. R.; Stephenson, J. C. *J. Chem. Phys.* **1986**, *85*, 5004. Li, M.; Owrutsky, J.; Sarisky, M.; Culver, J. P.; Yodh, A.; Hochstrasser, R. M. *J. Chem. Phys.* **1993**, *98*, 5499. Tokmakoff, A.; Zimdars, D.; Urdahl, R. S.; Francis, R. S.; Kwok, A. S.; Fayer, M. D. *J. Phys. Chem.* **1995**, *99*, 13310.
(15) Graener, H.; Dohlus, R.; Laubereau, A. *Chem. Phys. Lett.* **1987**, *140*, 306.
(16) Bonn, M.; Brugmans, M. J. P.; Kleyn, A. W.; van Santen, R. A.; Bakker, H. J. *J. Chem. Phys.* **1996**, *105*, 3431.Arrivo, S. M.; Heilweil, E. J. *J. Phys. Chem.* **1996**, *100*, 11975.
(17) Graener, H.; Seifert, G.; Laubereau, A. *Chem. Phys. Lett.* **1990**, *172*, 435.
(18) Laenen, R.; Rauscher, C.; Laubereau, A. *J. Phys. Chem.* **1997**, *A101*, 3201.
(19) Graener, H.; Seifert, G.; Laubereau, A. *Phys. Rev. Lett.* **1991**, *66*, 2092.
(20) Woutersen, S.; Emmerichs, U.; Bakker, H. J. *Science* **1997**, *278*, 658.
(21) Laenen, R.; Simeonidis, K.; Rauscher, C. *IEEE J. Sel. Top. Quantum Electron.* **1996**, *2*, 487.
(22) Laenen, R.; Simeonidis, K.; Laubereau, A. *J. Opt. Soc. Am.* **1998**, *B15*, 1213.
(23) Rauscher, C.; Laenen, R. *J. Appl. Phys.* **1997**, *81*, 2818.
(24) Press: W. H.; Flannery, B. P.; Teukolsky, S. A.; Vetterling, W. T. *Numerical Recipes*; Cambridge University Press: Cambridge, 1986.
(25) Laenen, R.; Rauscher, C.; Laubereau, A. *Phys. Rev. Lett.* **1998**, *80*, 2622.
(26) Band, Y. B. *Phys. Rev.* **1986**, *A34*, 326.
(27) Rahman, A.; Stillinger, F. H. *J. Chem. Phys.* **1971**, *55*, 3336.
(28) Ford, T. A.; Falk, M. *Can. J. Chem.* **1968**, *46*, 3579.
(29) Walrafen, G. E. *J. Solution Chem.* **1973**, *2*, 159.
(30) Stillinger, F. H. *Science* **1980**, **209**, 451.
(31) Walrafen, G. E. *J. Chem. Phys.* **1969**, **50**, 560.
(32) Giguere, P. A. *J. Chem. Phys.* **1987**, *87*, 4835.

(33) Sciortino, F.; Geiger, A.; Stanley, H. E. *Phys. Rev. Lett.* **1990**, *65*, 3452.
(34) Senior, W. A.; Verrall, R. E. *J. Phys. Chem.* **1969**, *73*, 4242 and references therein.
(35) Clarke, E. C. W.; Glew, D. N. *Can. J. Chem.* **1972**, *50*, 1655.
(36) Graener, H.; Lösch, T.; Laubereau, A. *J. Chem. Phys.* **1990**, *93*, 5365.
(37) Laenen, R.; Rauscher, C. *J. Chem. Phys.* **1997**, *106*, 8974.
(38) Finzi, J.; Hovis, F. E.; Panfilov, V. N.; Hess, P.; Moore, C. B. *J. Chem. Phys.* **1977**, *67*, 4053.
(39) Vodopyanov, K. L. *J. Chem. Phys.* **1991**, *94*, 5389.
(40) Laenen, R.; Rauscher, C. *Chem. Phys. Lett.* **1997**, *274*, 63.
(41) Graener, H.; Seifert, G.; Laubereau, A. *Chem. Phys.* **1993**, *175*, 193.
(42) Geiger, A.; Mausbach, P.; Schnitker, J.; Blumberg, R. L.; Stanley, H. E. *J. Phys.* **1984**, *45* (C7), 13.
(43) Luzar, A.; Chandler, D. *Nature* **1996**, *379*, 55.
(44) Marti, J.; Padro, J. A.; Guardia, E. *J. Chem. Phys.* **1996**, *105*, 639.
(45) Diraison, M.; Guissani, Y.; Leicknam, J.-Cl.; Bratos, S. *Chem. Phys. Lett.* **1996**, *258*, 348.
(46) Graener, H.; Ye, T.-Q.; Laubereau, A. *Phys. Rev.* **1990**, *B41*, 2597.